Nuclear Inst. and Methods in Physics Research, A 1048 (2023) 167924

Contents lists available at ScienceDirect

Nuclear Inst. and Methods in Physics Research, A

journal homepage: www.elsevier.com/locate/nima

Technical notes

Application of adaptive filtering algorithm to the stability problem for double crystal monochromator. Part I: Typical filtering algorithms

Yang Bai [a,b], Xuepeng Gong [a,*], Qipeng Lu [a], Yuan Song [a], Wanqian Zhu [c], Song Xue [c], Dazhuang Wang [a], Zhongqi Peng [a], Zhen Zhang [a]

[a] Changchun Institute of Optics, Fine Mechanics and Physics, Chinese Academy of Sciences, Changchun 130033, China
[b] University of Chinese Academy of Sciences, Beijing 100049, China
[c] Shanghai Advanced Research Institute, Chinese Academy of Sciences, Shanghai 201204, China

ARTICLE INFO

Keywords:
Synchrotron radiation sources
Double crystal monochromator
Typical filtering algorithms
Active vibration control

ABSTRACT

The double crystal monochromator (DCM) is one of the critical beamline devices in synchrotron radiation facilities. With the continuous improvement of the performance of the X-ray beamline of synchrotron radiation sources and the constant application of fourth-generation synchrotron radiation sources, higher requirements for the stability of the DCM have been introduced. Based on previous engineering experience, the LN_2 cooling system is the most critical factor affecting DCM's stability. In this paper, the vibration suppression performance of FxLMS (filter-x Least Mean Square), FxNLMS(filter-x Normalized Least Mean Square), FxSDLMS(filter-x Sign-Data Least Mean Square), FxSELMS(filter-x Sign-Error Least Mean Square) and FxSSLMS(filter-x Sign-Sign Least Mean Square) are verified under Bragg@12.66 KeV and Bragg@9 KeV operating conditions for the measured vibration signals of DCM at SSRF(Shanghai Synchrotron Radiation Facility). The results show that the FxNLMS algorithm has higher convergence accuracy, excellent vibration suppression performance, and the ability to counter unknown disturbances compared with other typical filtering algorithms.

1. Introduction

The new generation of synchrotron light sources currently under development is diffraction-limited light sources and free-electron lasers characterized by extremely high-quality coherence and high brightness, which have incredibly high coherence and very small focusing optical properties and enable in situ, dynamic and high-resolution scientific experiments [1–3]. The monochromator becomes one of the most critical components in the synchrotron radiation device, which converts synchrotron light into monochromatic light output under an ultra-high vacuum environment to obtain the monochromatic synchrotron light with specific energy required for scientific research. The monochromatic light with specific energy required for the application and its energy resolution is controlled and decided by the monochromator. Therefore, it is one of the most central optical instruments in synchrotron light applications [4,5]. In recent years, with the development of physics, chemistry, biology, and medicine, as well as advanced micro and Nano-manufacturing [6], large-scale integrated circuit chip manufacturing [7], and other fields, the performance of synchrotron radiation light source has put forward higher requirements [8]. Synchrotron radiation laboratories worldwide guarantee the stability of monochromators by optimizing the structure of DCM components, using vibration isolation materials, and optimizing the cooling system [9–13]. In recent years, with the rapid development of science and technology, active vibration control technology has been developed rapidly, its functions are becoming more and more perfect, and the control effect is better. It has been successfully applied to civil engineering structure seismic, vehicle structure damping, vibration isolation of ship hull structure, vibration control of precision mechanical equipment, and other fields [14]. Currently, the research of adaptive filtering algorithms mainly includes four aspects: methods based on Wiener filtering theory, methods based on least squares estimation, methods based on Kalman filtering theory, and methods based on neural networks. Although adaptive algorithms have been developed in the above four aspects, the LMS (Least Mean Square) algorithm, which is derived based on Wiener filtering, remains the most widely used adaptive filtering algorithm due to its simple structure, stable performance, low computational complexity, and easy implementation [15,16]. The control algorithm is based on the main idea of adaptive filtering, which has the advantages of simple structure, stable performance, low computational complexity, good convergence effect, and easy implementation. Therefore, it is widely used in AVC (active vibration control) and ANC (active noise control) [17].

In previous research, the numerical simulation results of vibration suppression by the FxLMS algorithm were initially presented with the

* Corresponding author.
E-mail address: gongxuepeng120@foxmail.com (X. Gong).

https://doi.org/10.1016/j.nima.2022.167924
Received 24 August 2022; Received in revised form 9 December 2022; Accepted 13 December 2022
Available online 17 December 2022

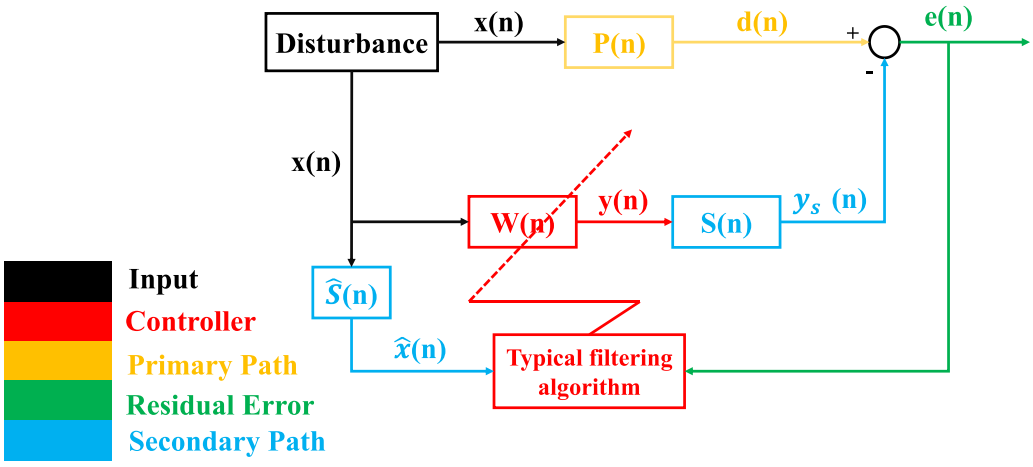

Fig. 1. The block diagram of a typical adaptive filtering algorithm.

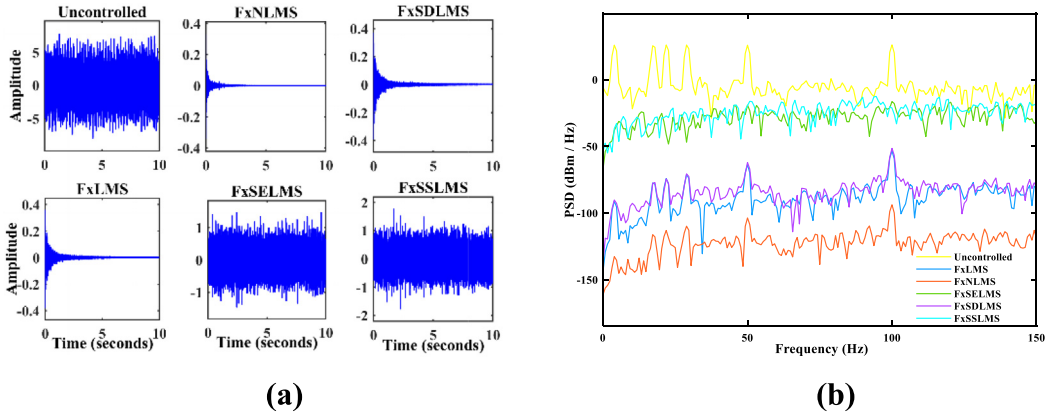

Fig. 2. Numerical simulation results. (a) Comparison of time-domain results. (b) Comparison of frequency-domain results.

flexible hinge of the crystal monochromator mechanism [18]. This paper verifies the vibration suppression performance of typical adaptive filtering algorithms (mainly FxLMS, FxNLMS, FxSDLMS, FxSELMS, and FxSSLMS) based on the measured vibration signals of DCM under Bragg@12.66KeV and Bragg@9KeV operating conditions at SSRF. The results show that typical adaptive filtering algorithms generally have good vibration suppression performance, resulting in an angle stability of 15 nrad or less in the pitch direction. In particular, the FxNLMS algorithm has superior vibration suppression performance, a faster convergence rate, and the ability to cope with uncertain perturbations.

2. Typical filtering algorithms

The LMS algorithm is widely used in signal processing and active noise reduction. The FxLMS (filter-xLMS algorithm) algorithm has the following advantages: (1) incorporating the practical needs of active noise cancellation; (2) introducing a secondary channel $S(n)$ in the LMS algorithm; (3) introducing a secondary channel modeling filter after the reference signal [19]. The block diagram of a typical adaptive filtering algorithm is shown in Fig. 1.

The power coefficient of the transversal filter at time n is:

$$W(n) = [w_1(n), w_2(n), \ldots, w_L(n)] \tag{1}$$

The signal input at the time n is:

$$X(n) = [x_1(n), x_2(n), \ldots, x_L(n)] \tag{2}$$

Where L is the filter order.

The expected signal is

$$d(n) = X(n) * P(n) \tag{3}$$

Where $P(n)$ is the primary path.

The reaction signal is

$$y_s(n) = y(n) * S(n) \tag{4}$$

The filter output is

$$y(n) = \sum_{l=0}^{L} w_l(n)\, x(n-l+1) \tag{5}$$

Substituting Eq. (5) into Eq. (4) is

$$y_s(n) = \sum_{l=0}^{L} w_l(n)\, \hat{x}(n-l+1) \tag{6}$$

The matrix form of Eq. (6) is

$$y_s(n) = W(n)X^T(n) \tag{7}$$

The output signal (filtered signal) of the secondary channel is

$$\hat{X}(n) = W(n) * \hat{S}(n) \tag{8}$$

The residual error signal is

$$e(n) = d(n) - y_s(n) = d(n) - W(n)X^T(n) \tag{9}$$

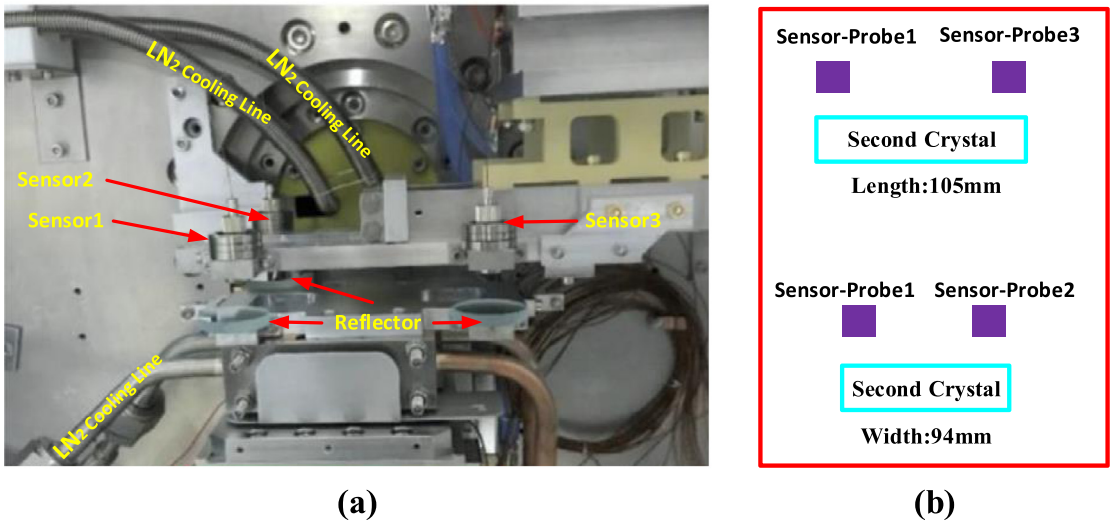

Fig. 3. Test diagram. (a) Actual measurement map [8]. (b) Test schematic.

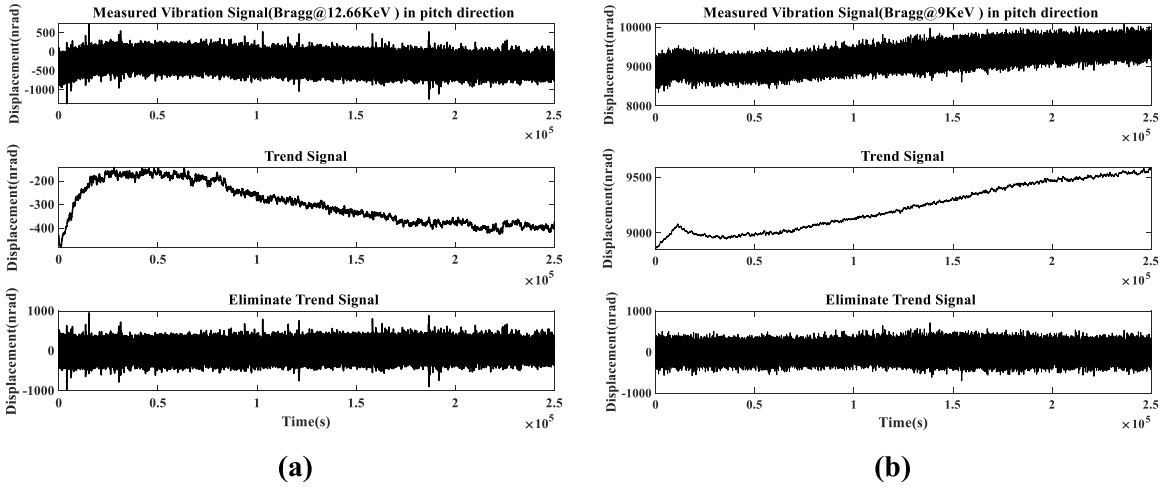

Fig. 4. The vibration test results. (a) Bragg@12.66KeV. (b) Bragg@9KeV.

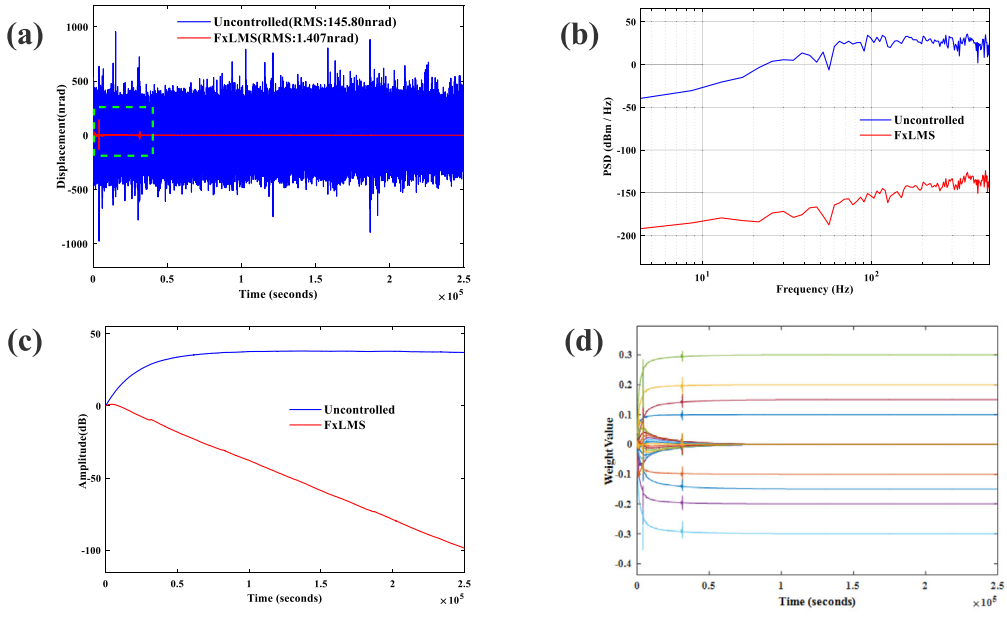

Fig. 5. FxLMS algorithm vibration suppression results. (a) Time-domain results (b) Frequency-domain results (c) Vibration level results (d) Weight iteration results.

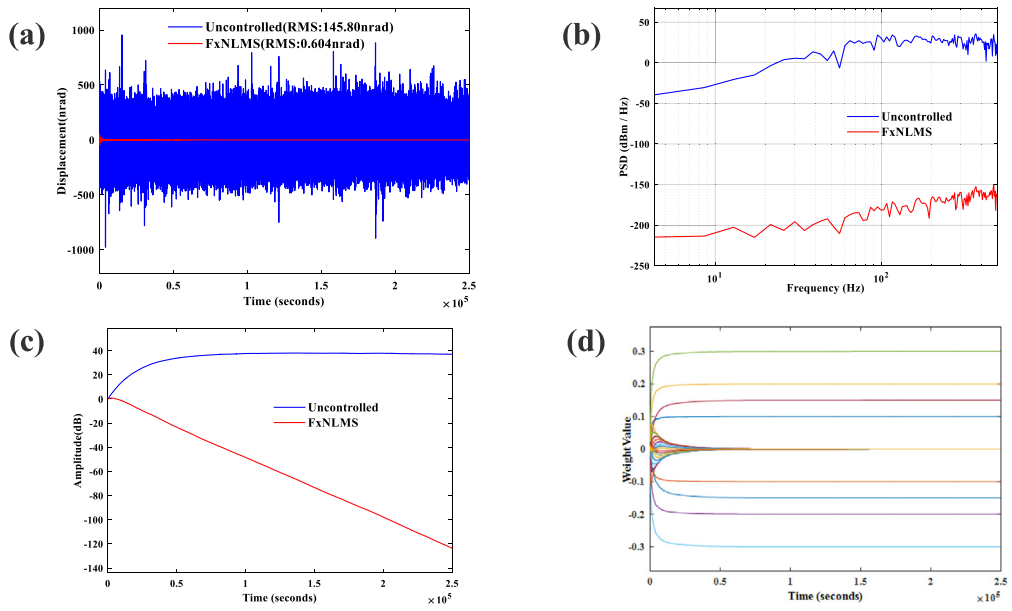

Fig. 6. FxNLMS algorithm vibration suppression results. (a) Time-domain results (b) Frequency-domain results (c) Vibration level results (d) Weight iteration results.

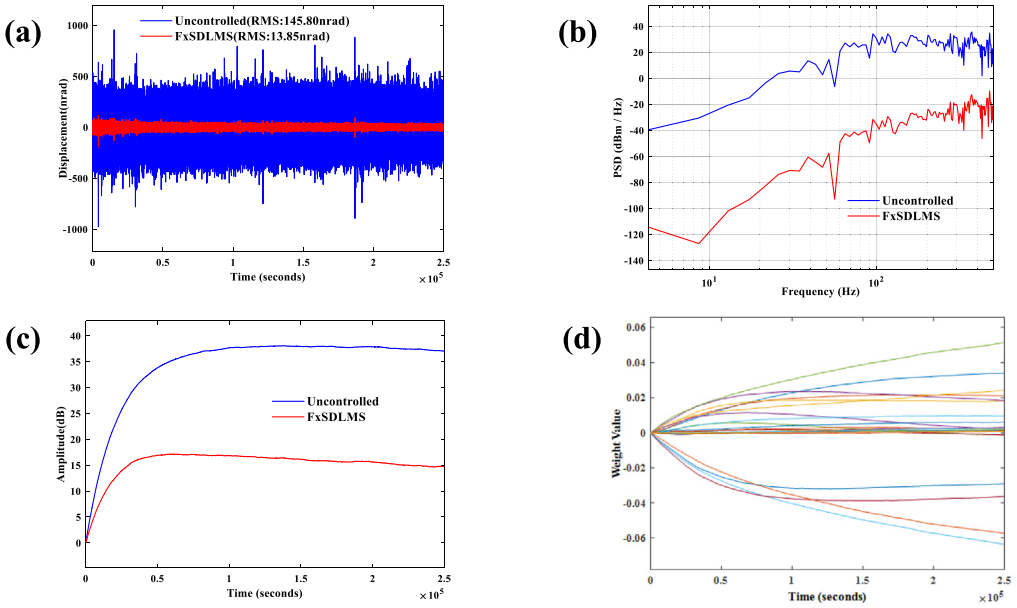

Fig. 7. FxSDLMS algorithm vibration suppression results. (a) Time-domain results (b) Frequency-domain results (c) Vibration level results (d) Weight iteration results.

The minimum mean square error criterion is expressed as the objective function:

$$\xi(n) = E(e^2(n)) = E(d^2(n)) - 2W^T E[d(n)\hat{X}(n)] + W^T E[X^T(n)\hat{X}(n)]W \tag{10}$$

Derivative of $\xi(n)$ with respect to W:

$$\nabla(n) = \frac{\partial E(\xi(n))}{\partial w} = -2E[e(n)X(n)] \tag{11}$$

The gradient vector is zero when the filter power coefficients reach to be the optimal solution.

The filter power factor equation is

$$W(n+1) = W(n) - \mu\nabla(n) \tag{12}$$

Where μ is the convergence factor.

The gradient $\hat{\nabla}(n)$ of a single error sample squared is taken as an estimate of $\nabla(n)$ [20], is given by

$$\hat{\nabla}(\mathrm{n}) = -2\mathrm{e}(\mathrm{n})\hat{X}(n) \tag{13}$$

Eq. (12) can be written as

$$W(n+1) = W(n) + 2\mu\mathrm{e}(\mathrm{n})\hat{X}(n) \tag{14}$$

The convergence factor in the LMS algorithm determines whether the adaptive process converges and how fast it converges. It also determines the size of the stability error value [21]. From Eq. (14), the energy of the reference signal affects the value of the convergence coefficient. When the reference signal changes too fast or the exact energy value cannot be estimated, the convergence coefficient is challenging to choose. Therefore, the iterative formula for the weight coefficients

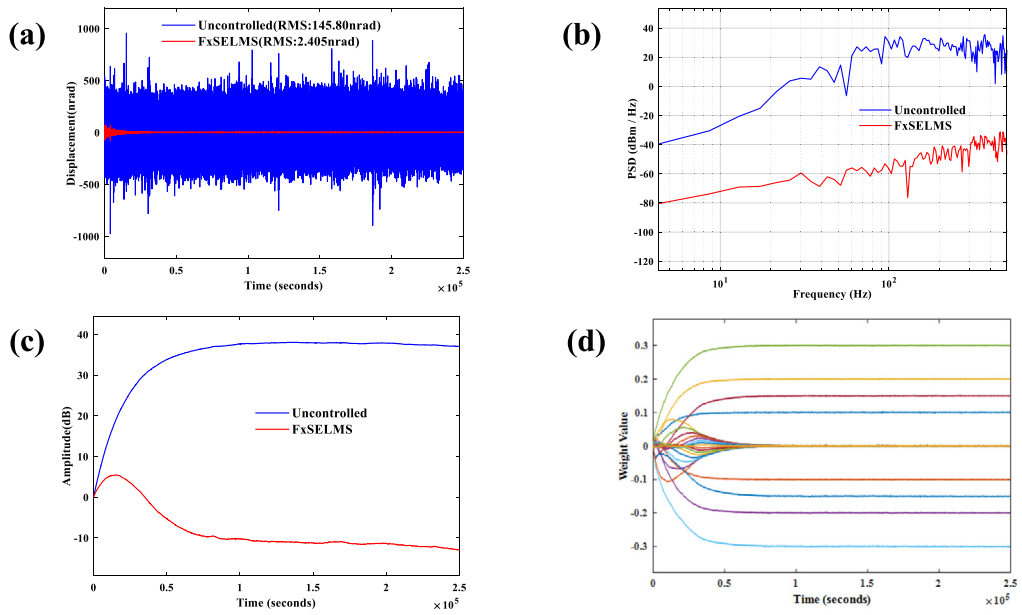

Fig. 8. FxSELMS algorithm vibration suppression results. (a) Time-domain results (b) Frequency-domain results (c) Vibration level results (d) Weight iteration results.

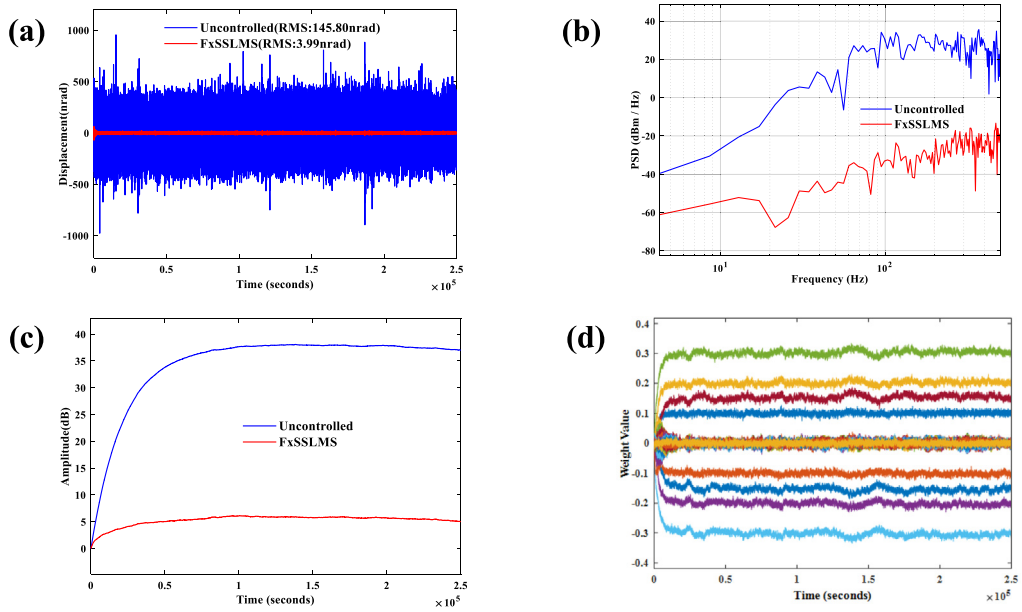

Fig. 9. FxSSLMS algorithm vibration suppression results. (a) Time-domain results (b) Frequency-domain results (c) Vibration level results (d) Weight iteration results.

of the NLMS algorithm is

$$W(n+1) = W(n) + e(n)X(n)\frac{2\mu_0}{X^T X(n) + \varepsilon} \tag{15}$$

Where $0 < \mu_0 < 2$.

The iterative formula for the weight coefficients of the SELMS algorithm is

$$W(n+1) = W(n) + \mu sign(e(n))\hat{X}(n) \tag{16}$$

The iterative formula for the weight coefficients of the SDLMS algorithm is

$$W(n+1) = W(n) + \mu e(n) sign(X(n)) \tag{17}$$

The iterative formula for the weight coefficients of the SSLMS algorithm is

$$W(n+1) = W(n) + \mu sign(e(n)) sign(X(n)) \tag{18}$$

Numerical simulations were performed to verify the effectiveness of typical filtering algorithms. The interference source comprises Gaussian white noise and sinusoidal signal (frequency: 4 Hz/17.5 Hz/22 Hz/29.1 Hz/50 Hz/100 Hz). The frequency of the liquid nitrogen cooling circulation pump is 22 Hz; the natural frequency of the crystal clamping mechanism is 29.1 Hz; the frequency of the marble support platform is 17.5 Hz; the disturbance frequency of the liquid nitrogen pipeline fixed by external suspension is 4 Hz; the industrial frequency noise is 50 Hz; the frequency of servo system is 100 Hz [22]. The control system is established based on the MATLAB/Simulink platform, and the results are shown in Fig. 2. From Fig. 2, it is clear that FxLMS, FxNLMS, FxSDLMS, FxSELMS, and FxSSLMS algorithms have higher convergence accuracy and better control performance. It can be found in Fig. 2(b) that the signal amplitude decreases at frequencies 4 Hz/17.5 Hz/22 Hz/29.1 Hz/50 Hz/100 Hz, in which the FxNLMS algorithm is the most obvious. From Eq. (15), the convergence factor

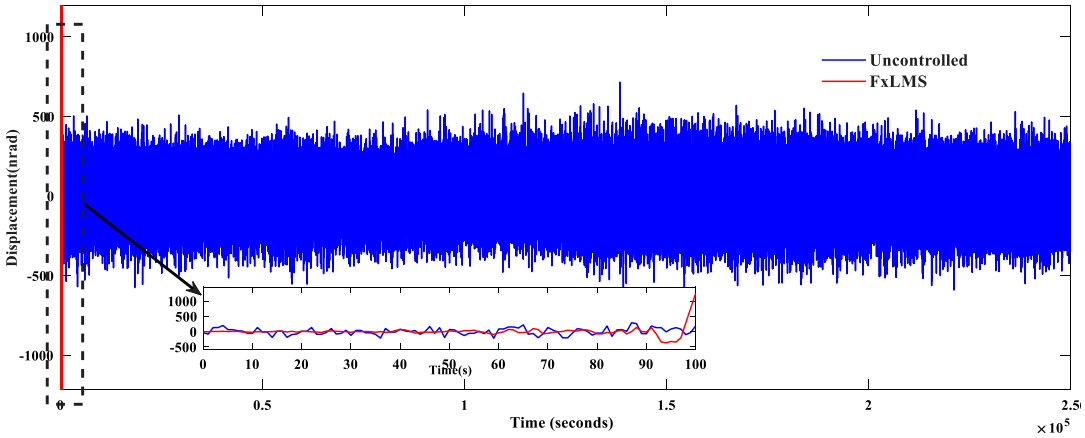

Fig. 10. FxLMS algorithm vibration suppression results.

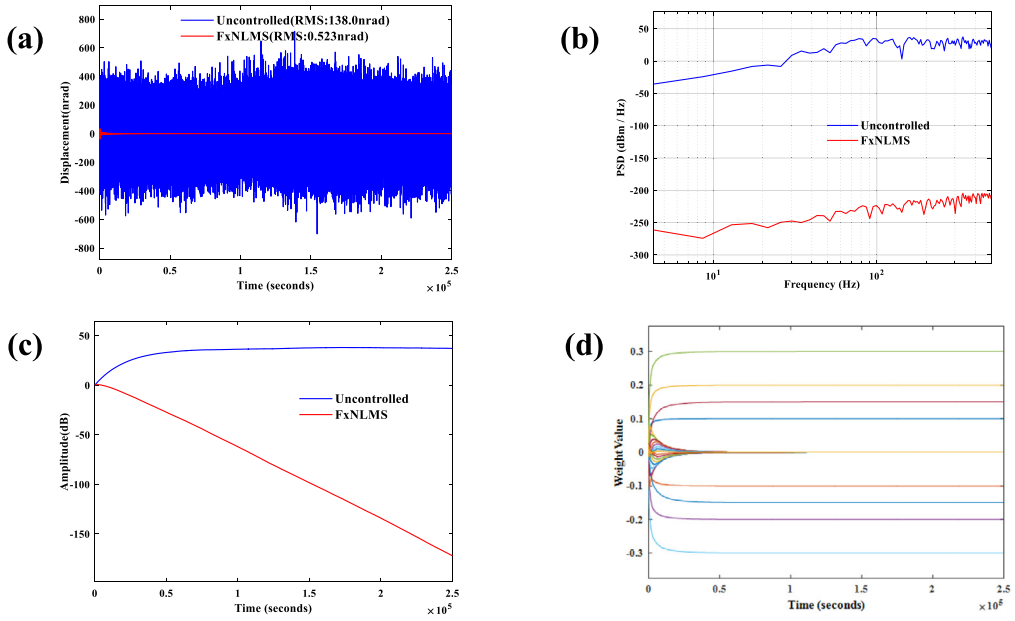

Fig. 11. FxNLMS algorithm vibration suppression results. (a) Time-domain results (b) Frequency-domain results (c) Vibration level results (d) Weight iteration results.

of the normalized LMS algorithm (NLMS) is no longer fixed. Instead, it varies with time, and the adaptive capability is significantly enhanced.

3. Case verification

The vibration test device was constructed to obtain the vibration signals of different working conditions of the double crystal monochromator in the Shanghai synchrotron radiation facility (SSRF), and the actual test diagram is shown in Fig. 3. The type of sensor used for the vibration test is German attocube laser displacement sensor. Elimination of the trend term (sensor offset) is performed by the sgolayfilt filtering algorithm. The vibration test results under Bragg@12.66KeV and Bragg@9KeV working conditions are shown in Fig. 4.

The interferometer is capable of measuring with a resolution of 1 pm and a bandwidth of 10 MHz, as well as being suitable for UHV and cryogenic conditions. Three sensor probes were used in the test work, each mounted at a different position on the second crystal; three reflectors were attached to the same places on the first crystal. The sensors are divided into two groups: sensor one and sensor three are arranged in the pitch direction at a distance of 105 mm; sensor one and sensor two are set in the roll direction at 94 mm. During the whole test, the tank pressure of the liquid nitrogen circulation unit was 2 Bar; the bypass valve switching volume was 60%; the operating frequency of the liquid nitrogen circulation pump was 22 Hz; the flow rate of the liquid nitrogen cooling circuit was about 3.2 L/min (the flow rate of the liquid nitrogen circuit varies slightly at different scanning energies); the DCM pressure was maintained at 8.0E−09 Torr; the temperature of SSRF experiment hall was strictly controlled at 25 ± 0.5 °C.

3.1. Case 1: Bragg@12.66KeV

Measured vibration signals from crystal monochromator under Bragg@12.66KeV conditions are applied to verify the accuracy of FxLMS, FxNLMS, FxSDLMS, FxSELMS, and FxSSLMS algorithms. In order to reduce the computational complexity while not compromising the vibration suppression effect, the filter length is set to 24 charges. The vibration suppression time-domain, frequency-domain results, vibration level results, and weight iteration results of FxLMS, FxNLMS, FxSDLMS, FxSELMS, and FxSSLMS algorithms are shown in Figs. 5–9 as follows.

From the time-domain results of Figs. 5(a), 6(a), 7(a), 8(a), and 9(a), the FxLMS, FxNLMS, FxSDLMS, FxSELMS, and FxSSLMS algorithms reduce the angular displacement by about 99.03%, 99.59%, 90.50%, 98.35% and 97.26% as respectively. In particular, the minimum angular displacement in the Pitch direction is 0.604 nrad below 15 nrad;

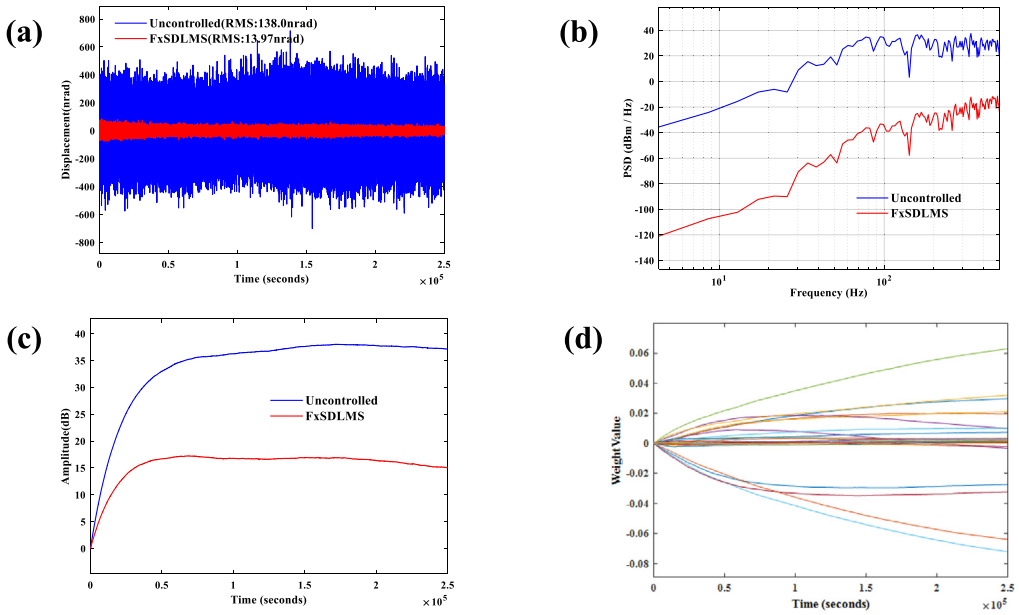

Fig. 12. FxSDLMS algorithm vibration suppression results. (a) Time-domain results (b) Frequency-domain results (c) Vibration level results (d) Weight iteration results.

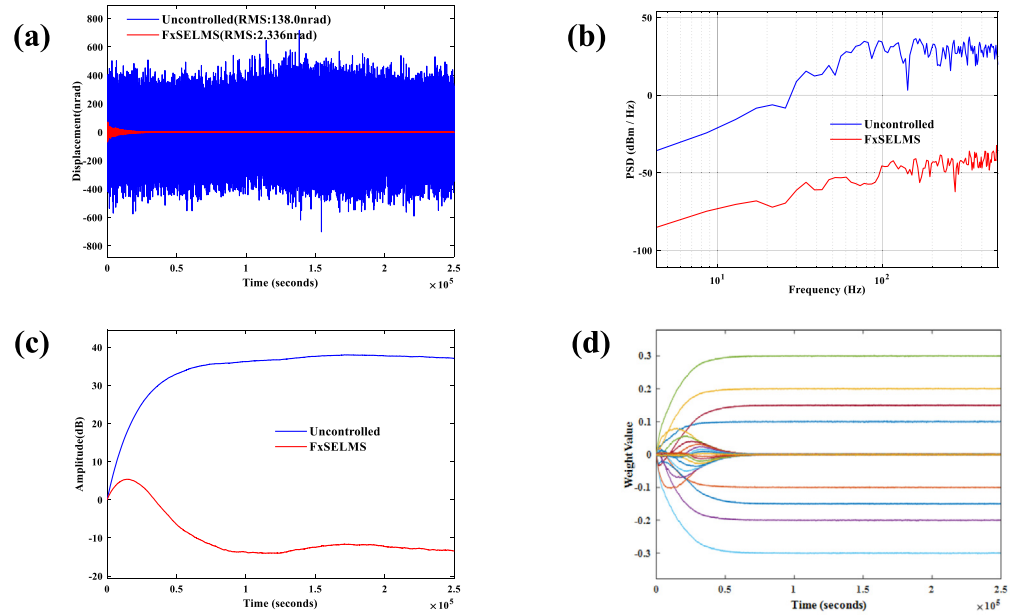

Fig. 13. FxSELMS algorithm vibration suppression results. (a) Time-domain results (b) Frequency-domain results (c) Vibration level results (d) Weight iteration results.

the results in the frequency-domain of Figs. 5(b), 6(b), 7(b), 8(b) and 9(b) show that the vibration suppression is excellent. The vibration level results from Figs. 5(c), 6(c), 7(c), and Figs. 8(c) and 9(c) vibration level results can more intuitively demonstrate the vibration suppression capability of the typical adaptive filtering algorithm. From the results of the weight iterations in Figs. 5(d), 6(d), 7(d), 8(d), and 9(d), it can be seen that the filtering algorithms all converge approximately; in particular, the FxNLMS algorithm converges with the highest speed and accuracy; on the contrary, the FxSDLMS algorithm converges slowly in parts of the weights, and the FxSSLMS algorithm fluctuates more in the weight iteration process. A few spikes in the residual signal can be found in the green wireframe of Fig. 5(a). Similar problems exist in the FxSDLMS, FxSELMS, and FxSSLMS algorithms, which indicates that the FxLMS, FxSDLMS, FxSELMS, and FxSSLMS algorithms are insensitive to unknown disturbances and have poor adaptive ability to suppress unknown perturbations. From Figs. 6(a), 6(b), 6(c), and 6(d), it is known that the FxNLMS algorithm has high convergence accuracy, high convergence rate, and high adaptive ability to cope with uncertain perturbations.

3.2. Case 2: Bragg@9KeV

In this case, the vibration suppression time-domain, frequency-domain results, vibration level results, and weight iteration results of FxLMS, FxNLMS, FxSDLMS, FxSELMS, FxSSLMS algorithms are shown in Figs. 10–14 as follows.

From Fig. 10, the FxLMS algorithm control fails, and divergence occurs in the Bragg@9KeV operating condition. From Figs. 5 and 10, it can be found that the FxLMS algorithm convergence step (convergence coefficient) is a very critical quantity that determines whether the adaptive process converges or diverges, the degree of convergence, and the magnitude of the steady-state error of the adaptive process. The number

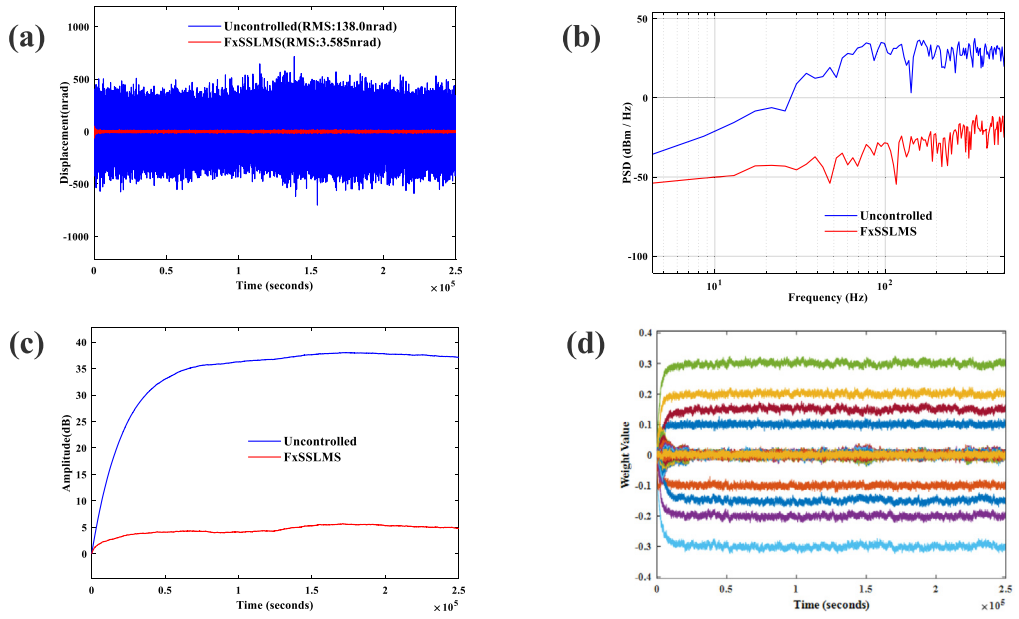

Fig. 14. FxSSLMS algorithm vibration suppression results. (a) Time-domain results (b) Frequency-domain results (c) Vibration level results (d) Weight iteration results.

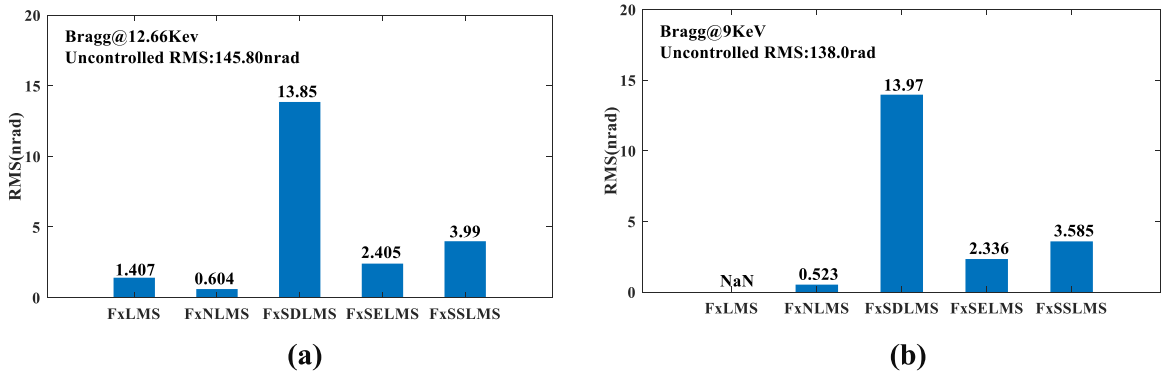

Fig. 15. Comparison of stability index results under Bragg@12.66KeV and Bragg@9KeV working conditions. (a) Bragg@12.66KeV (b) Bragg@9KeV.

of filter taps and the input signal size determines the convergence step. Since the convergence coefficient of the FxLMS algorithm is a fixed value, the FxLMS algorithm cannot perform its adaptive properties in some cases where the step parameters cannot be determined.

From the time domain results of Figs. 11(a), 12(a), 13(a), and 14(a), it is known that the FxNLMS, FxSDLMS, FxSELMS, and FxSSLMS algorithms reduce the angular displacement by about 99.62%, 89.88%, 98.31%, 97.40% as respectively, and can keep the angular displacement below 15 nrad; in particular, the minimum value of the angular displacement in the Pitch direction is about 0.523 nrad. From the Frequency-domain results of Figs. 11(b), 12(b), 13(b), and 14(b) and the vibration level results of Figs. 11(c), 12(c), 13(c) and 14(c), the vibration suppression effect is more intuitively presented. From the results of the iterative weights of the FxNLMS algorithm in Fig. 11(d), it is known that the FxNLMS algorithm converges quickly, and the consequences are more stable during the iterative process. Conversely, from the iterative results of the FxSDLMS algorithm weights in Fig. 12(d) and the iterative results of the FxSSLMS algorithm weights in Fig. 14(d), we know that the convergence rate is slower in the iterative process and the FxSSLMS algorithm weights fluctuate more in the convergence process. In general, the FxSELMS algorithm is more stable, as known from the iterative results of FxSELMS weights in Fig. 13(d). However, the convergence speed is slower compared to the FxNLMS algorithm.

4. Conclusion

This paper mainly verifies the vibration suppression capability of FxLMS, FxNLMS, FxSDLMS, FxSELMS, and FxSSLMS algorithms for measured signals under Bragg@12.66KeV and Bragg@9KeV working conditions. The vibration suppression indexes of DCM under Bragg@12.66KeV and Bragg@9KeV working conditions are shown in Fig. 15. The results show that the adaptive filter has an excellent vibration suppression effect under Bragg@12.66KeV and Bragg@9KeV. However, control failure also occurs under specific working conditions. In particular, the FxNLMS algorithm shows exceptional adaptive ability, convergence speed, and convergence accuracy. This work has important practical significance for developing high-stability DCM.

Declaration of competing interest

The authors declare that they have no known competing financial interests or personal relationships that could have appeared to influence the work reported in this paper.

Thanks to the support of the researchers at SSRF (Shanghai Synchrotron Radiation Facilities of China).

Data availability

The authors do not have permission to share data.

Acknowledgments

The work is supported by National Natural Science Foundation of China (No. 61974142, No. 62104224) and "Xu-Guang" Talent Program of Changchun Institute of Optics, Fine Mechanics and Physics (CIOMP), Chinese Academy of Sciences (CAS), China (E01672Y6Q0).

References

[1] Emma, et al., First lasing of the LCLS at l.5A, 2009.
[2] Donald, et al., Review of third and next generation synchrotron light sources, 2005.
[3] J. Feldhaus, et al., XFEL review, 2005.
[4] N.X. Wang, Y.Q. Wei, et al., Study of stress deformation and thermal retardation in monochromator crystals, High Energy Phys. Nucl. Phys. Sci. 26 (11) (2002) 1189–1190 (in Chinese).
[5] Xu Zhaoyin, Pan Guoqiang, X-ray diffraction and scattering beam line design, J. Univ. Sci. Technol. China 29 (2) (1999) 181–182 (in Chinese).
[6] Di Liang, John E. Bowers, Recent progress in heterogeneous III-V-on-silicon photonic integration, Light Adv. Manuf. 2 (1) (2021) 59–83.
[7] Lin Zhu, Yong-Lai Zhang, Hong-Bo Sun, Miniaturizing artificial compound eyes based on advanced micro nanofabrication techniques, Light Adv. Manuf. 2 (1) (2021) 84–100.
[8] Y. Fan, H. Qin, et al., Angular stability measurement of a cooled double-crystal monochromator at SSRF, Nucl. Instrum. Methods Phys. Res. A 983 (2020) 164636.
[9] Y. Dabin, L. Zhang, D. Martin, et al., The concrete slab studies for the ESRF upgrade beam lines, in: The 7th International Conference on Mechanical Engineering Design of Synchrotron Radiation Equipment and Instrumentation, MEDSI 2012, Shanghai, 2012.
[10] Roland Barrett, et al., New generation mirror systems for the ESRF upgrade beam lines, J. Phys. Conf. Ser. (2013).
[11] Noriyuki Igarashi, Kazuyuki Ikuta, Toshinobu Miyoshi, et al., X-ray beam stabilization at BL-17A, the protein micro crystallography beam line of the photon factor, J. Synchrotron Radiat. 15 (2008) 292–296.
[12] H. Yamazaki, H. Ohashi, Y. Senba, et al., Improvement in stability of spring-8 X-ray monochromators with cryogenic-cooled silicon crystals, J. Phys. Conf. Ser. (2013).
[13] Hiroshi Yamazaki, et al., Challenges toward 50 nrad-stability of X-rays for a next generation light source by refinements of SPring-8 standard monochromator with cooled Si crystals, AIP Conf. Proc., 2054, 060018.
[14] M. Zhao, H.T. Zhou, et al., Mechanical Vibration and Noise Science, Science Press, Beijing, 2004, p. 1.
[15] N. Li, Research and Application of Convergence Performance of LMS Adaptive Filtering Algorithm, Harbin Engineering University, 2009 (in Chinese).
[16] Qi Haichao, Software Development and Experimental Study of Vibration Active Control Simulation Based on LMS Adaptive Filtering Algorithm, Harbin Engineering University, 2012 (in Chinese).
[17] W. Li, et al., Hybrid feedback PID–FxLMS algorithm for active vibration control of cantilever beam with piezoelectric stack actuator, J. Sound Vib. (2021).
[18] Bai Yang, et al., Active vibration control method of double crystal monochromator of P2 protein crystallography beam line at SSRF, Nucl. Instrum. Methods Phys. Res. A (2021) 1019.
[19] D.R. Morgan, An analysis of multiple correlation cancellation with a filter in the auxiliary path, IEEE Trans. Acoust. Speech Signal Process. (ASSP-28) (1980) 454–467.
[20] J.C. Burgress, Active adaptive sound control in a duct: A computer simulation, J. Acoust. Soc. Am. 70 (3) (1981) 715–726.
[21] Lin Guo, Yun-Sheng Yan, Digital Signal Processor I Architecture, Implementation and Applications, Tsinghua University Press, Beijing, 2005 (in Chinese).
[22] Fan Yichen, Study on the Stability Testing Technique of Liquid Nitrogen-Cooled Biocrystal Monochromator, University of Chinese Academy of Sciences (Shanghai Institute of Applied Physics, Chinese Academy of Sciences, 2020 (in Chinese).